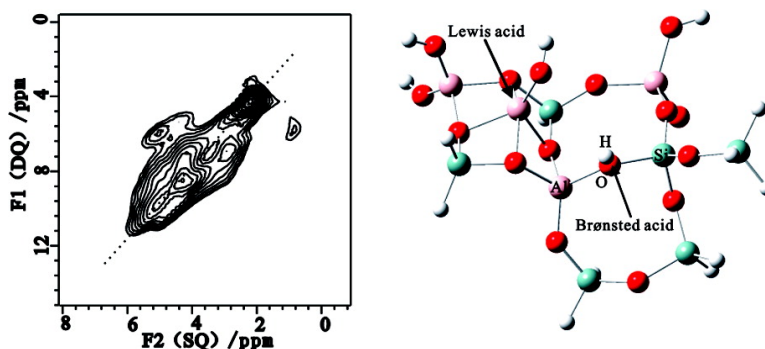


## Brønsted/Lewis Acid Synergy in Dealuminated HY Zeolite: A Combined Solid-State NMR and Theoretical Calculation Study

Shenhui Li, Anmin Zheng, Yongchao Su, Hailu Zhang, Lei Chen, Jun Yang, Chaohui Ye, and Feng Deng

*J. Am. Chem. Soc.*, **2007**, 129 (36), 11161-11171 • DOI: 10.1021/ja072767y • Publication Date (Web): 17 August 2007

Downloaded from <http://pubs.acs.org> on February 14, 2009



### More About This Article

Additional resources and features associated with this article are available within the HTML version:

- Supporting Information
- Links to the 6 articles that cite this article, as of the time of this article download
- Access to high resolution figures
- Links to articles and content related to this article
- Copyright permission to reproduce figures and/or text from this article

[View the Full Text HTML](#)

## Brønsted/Lewis Acid Synergy in Dealuminated HY Zeolite: A Combined Solid-State NMR and Theoretical Calculation Study

Shenhui Li, Anmin Zheng, Yongchao Su, Hailu Zhang, Lei Chen, Jun Yang, Chaohui Ye, and Feng Deng\*

Contribution from the State Key Laboratory of Magnetic Resonance and Atomic and Molecular Physics, Wuhan Center for Magnetic Resonance, Wuhan Institute of Physics and Mathematics, The Chinese Academy of Sciences, Wuhan 430071, China

Received April 20, 2007; E-mail: dengf@wipm.ac.cn

**Abstract:** The Brønsted/Lewis acid synergy in dealuminated HY zeolite has been studied using solid-state NMR and density function theory (DFT) calculation. The  $^1\text{H}$  double quantum magic-angle spinning (DQ-MAS) NMR results have revealed, for the first time, the detailed spatial proximities of Lewis and Brønsted acid sites. The results from  $^{13}\text{C}$  NMR of adsorbed acetone as well as DFT calculation demonstrated that the Brønsted/Lewis acid synergy considerably enhanced the Brønsted acid strength of dealuminated HY zeolite. Two types of Brønsted acid sites (with enhanced acidity) in close proximity to extra-framework aluminum (EFAL) species were identified in the dealuminated HY zeolite. The NMR and DFT calculation results further revealed the detailed structures of EFAL species and the mechanism of Brønsted/Lewis acid synergy. Extra-framework  $\text{Al}(\text{OH})_3$  and  $\text{Al}(\text{OH})^{2+}$  species in the supercage and  $\text{Al}(\text{OH})^{2+}$  species in the sodalite cage are the preferred Lewis acid sites. Moreover, it is the coordination of the EFAL species to the oxygen atom nearest the framework aluminum that leads to the enhanced acidity of dealuminated HY zeolite though there is no direct interaction (such as the hydrogen-bonding) between the EFAL species and the Brønsted acid sites. All these findings are expected to be important in understanding the roles of Lewis acid and its synergy with the Brønsted acid in numerous zeolite-mediated hydrocarbon reactions.

### Introduction

Faujasite zeolite is important in the catalytic cracking, hydrocracking, and isomerization reactions in the petrochemical industry and its widespread application is mainly attributed to its acid-catalyzed activity. A mild hydrothermal treatment of faujasite-type Y zeolite usually results in a partial release of aluminum from the zeolite framework and the formation of an extra-framework aluminum (EFAL) species, which improves not only the thermal stability but also the catalytic activity of the zeolite.<sup>1–3</sup> The oxoaluminum cations, such as  $\text{AlO}^+$ ,  $\text{Al}(\text{OH})_2^+$ , and  $\text{AlOH}^{2+}$ , and some neutral species such as  $\text{AlOOH}$  and  $\text{Al}(\text{OH})_3$  are proposed to be the EFAL species though the detailed structures are not certain.<sup>4</sup> The favorable influence of dealumination on the catalytic properties of HY zeolite has been known for many years. The increased acidity of the zeolite due to the reduction of the number of framework Al as well as the presence of EFAL species has been attributed to the beneficial effect. However, the effect of EFAL species on the catalytic activity is complicated and remains to be fully understood. Three hypotheses have been proposed to explain

the favorable effect: (i) some EFAL species themselves are catalytic sites (Lewis acid sites);<sup>5</sup> (ii) the presence of EFAL species stabilizes the negative charges on the lattice after the removal of acidic proton;<sup>6</sup> (iii) there is a synergistic effect between EFAL species and nearby Brønsted acid sites.<sup>7–13</sup>

The existence of Brønsted/Lewis acid synergy is still actively debated in the literature. Although direct experimental evidence was absent, some authors proposed the Brønsted/Lewis acid synergy (interaction) to interpret the higher catalytic performance of dealuminated HY zeolite.<sup>7–13</sup> Microdatos et al.<sup>7</sup> suggested that the superacid sites in dealuminated zeolites resulted from the interactions between protonic sites and polymeric oxoaluminum deposited in the zeolite voids. Guisnet et al.<sup>8</sup> proposed that the inductive influence of the Lewis acid sites on the protonic sites of the zeolite was responsible for the promoting effect on the rates of isomerization, cracking, and hydrogen transfer in dealuminated HY. Corma et al.<sup>10</sup> showed that the cationic species of EFAL compensated the charge deficiency

- (1) DeCanio, S. J.; Sohn, J. R.; Fritz, P. O.; Lunsford, J. H. *J. Catal.* **1986**, *101*, 132–141.
- (2) Sohn, J. R.; DeCanio, S. J.; Fritz, P. O.; Lunsford, J. H. *J. Phys. Chem.* **1986**, *90*, 4847–4851.
- (3) Beyerlein, R. A.; McVicker, G. B.; Yacullo, L. N.; Ziemiak, J. *J. Phys. Chem.* **1988**, *92*, 1967–1970.
- (4) Shannon, R. D.; Gardner, K. H.; Staley, R. H.; Bergeret, G.; Gallezot, P.; Auroux, A. *J. Phys. Chem.* **1985**, *89*, 4778–4788.

- (5) Carvajal, R.; Chu, P.; Lunsford, J. H. *J. Catal.* **1990**, *125*, 123–131.
- (6) Lunsford, J. H. *J. Phys. Chem.* **1968**, *72*, 4163–4168.
- (7) Microdatos, C.; Barthomeuf, D. *J. Chem. Soc., Chem. Commun.* **1981**, *2*, 39–40.
- (8) Wang, Q. L.; Giannetto, G.; Guisnet, M. *J. Catal.* **1991**, *130*, 471–482.
- (9) Fritz, P. O.; Lunsford, J. H. *J. Catal.* **1989**, *118*, 85–98.
- (10) Corma, A.; Fornés, V.; Rey, F. *Appl. Catal.* **1990**, *59*, 267–274.
- (11) Beyerlein, R. A.; McVicker, G. B.; Yacullo, L. N.; Ziemiak, J. *J. Phys. Chem.* **1988**, *92*, 1967–1970.
- (12) Lónyi, F.; Lunsford, J. H. *J. Catal.* **1992**, *136*, 566–577.
- (13) Batamack, P.; Morin, C. D.; Vincent, R.; Fraissard, J. *Micropor. Mater.* **1994**, *2*, 525–535.

of bridging hydroxyl groups and increased the acidity strength of steamed HY. With  $^1\text{H}$  broad-line NMR at 4 K and  $^1\text{H}$  MAS NMR at 300 K, Batamack et al.<sup>13</sup> proposed that the Brønsted/Lewis acid synergy that was mediated through adsorbed water molecules was responsible for the increase in the number of hydroxonium ions in dealuminated HY. On the other hand, Remy et al.<sup>14</sup> suggested that the strength of the acid sites associated with tetrahedral framework Al atoms in dealuminated HY was not influenced by the other types of Al. Biaglow et al.<sup>15</sup> also demonstrated that there was no evidence for the presence of special sites in steamed faujasites, and the enhanced cracking activities were not due to the enhanced acidity of the hydroxyl sites.

Solid-state NMR has been proven to be a powerful tool to characterize the nature of different acid sites on various solid acids, including zeolites.  $^1\text{H}$  MAS NMR can provide structural information about various hydroxyl groups.<sup>16,17</sup> Adsorption of the probe molecules (such as  $2\text{-}^{13}\text{C}$ -acetone, deuterated pyridine, and trimethylphosphine) on acidic catalysts, in combination with magic angle spinning (MAS), is one of the widely used methods to characterize the solid acidity as well as the interactions between probe molecules and acid sites.<sup>18–20</sup> In particular,  $^{13}\text{C}$  MAS NMR of adsorbed  $2\text{-}^{13}\text{C}$ -acetone can be used as a scale to measure the relative acid strength of various solid catalysts.<sup>21,22</sup>

Theoretical calculation can provide useful information on the acid strength, the interaction between probe molecules and acid centers as well as the reaction transition state formed on solid acids. For example, Haw et al.<sup>23–25</sup> calculated the proton affinity and the  $^{13}\text{C}$  chemical shift of adsorbed  $2\text{-}^{13}\text{C}$ -acetone in order to measure the acid strength of various solid acids. Our previous studies have also demonstrated that the combination of solid-state NMR experiment with theoretical calculation can be an efficient approach to study the solid acid catalysts.<sup>26–28</sup> In a recent theoretical calculation study of the EFAL species in ultrastable Y zeolite, Mota et al.<sup>29,30</sup> found that various EFAL species were connected to the oxygen atoms nearest to framework aluminum in different forms and the EFAL species

reduced the acid strength of the framework hydroxyl groups (no Brønsted/Lewis acid synergy was found). In some cases, a strong hydrogen-bond interaction was found between the EFAL species and the Brønsted acid site.<sup>30</sup> If this were true, the  $^1\text{H}$  chemical shift of the Brønsted acid site would move significantly to the low field because of the hydrogen-bond interaction. However, NMR experiments demonstrated that the  $^1\text{H}$  chemical shift of the Brønsted acid site remained almost unchanged before and after the dealumination of HY zeolite.<sup>31</sup>

In this work,  $^1\text{H}$  DQ MAS solid-state NMR spectroscopy was employed to investigate the spatial proximities between Lewis and Brønsted acid sites in dealuminated HY zeolite, and  $2\text{-}^{13}\text{C}$ -acetone was used as a probe to measure the acid strength of the zeolite. Theoretical calculations were also carried out on several selected models that were proposed based on our NMR experimental results to study the Brønsted/Lewis acid synergy. The good agreement between the theoretical calculations and the experimental observations revealed the detailed structures of Lewis acid sites (EFAL species) and their synergy with Brønsted acid sites in dealuminated HY zeolite.

## Experimental and Computational Methods

**Sample Preparation.** Zeolite Na-Y ( $n_{\text{Si}}/n_{\text{Al}} = 2.8$ ) was exchanged in an  $1.0\text{ mol g}^{-1}$  aqueous solution of  $\text{NH}_4\text{Cl}$  at 353 K for 4 h. The process was repeated four times. The obtained zeolite  $\text{NH}_4\text{Y}$  was washed with distilled water until it became chloride-free. Subsequently, the powder material was dried in air at 353 K for 12 h. To prepare HY zeolite, the obtained  $\text{NH}_4\text{Y}$  sample was deaminated and dehydrated on a vacuum line, which could significantly avoid the dealumination of the zeolite framework (only the 4-coordinated  $^{27}\text{Al}$  signal was observed in the  $^{27}\text{Al}$  MAS NMR spectrum). The temperature was raised from room temperature to 383 K at a rate of 1 K/min and then from 383 to 673 K at a rate of 1.6 K/min. The sample was kept at 673 K for about 8 h under a pressure below  $10^{-3}$  Pa and then flame-sealed. Dealuminated HY zeolite was prepared as follows: the  $\text{NH}_4\text{Y}$  sample was placed in a quartz crucible in a tube furnace and calcined at 773 K in air for 4 h (the temperature was raised from room temperature to 773 K at a rate of 3 K/min). Prior to NMR experiments, the dealuminated HY samples were placed in glass tubes and dehydrated at 623 K under a pressure below  $10^{-3}$  Pa for 10 h on a vacuum line. After the dehydrated samples cooled to room temperature, a known amount of  $2\text{-}^{13}\text{C}$ -acetone was introduced and frozen by liquid  $\text{N}_2$ . Finally, the samples were flame-sealed. The adsorption of  $2\text{-}^{13}\text{C}$ -acetone onto the HY zeolite was carried out in a similar way. The sealed samples were transferred into a  $\text{ZrO}_2$  rotor (tightly sealed by a Kel-F cap) under a dry nitrogen atmosphere in a glove box. The Si/Al ratios, determined by  $^{29}\text{Si}$  MAS NMR, are 2.8 and 3.5 for the obtained HY and dealuminated HY zeolites, respectively.

**NMR Measurements.** All NMR experiments were carried out on a Varian Infinityplus-400 spectrometer at resonance frequencies of 400.1, 104.3, 100.6, and 79.5 MHz for  $^1\text{H}$ ,  $^{27}\text{Al}$ ,  $^{13}\text{C}$ , and  $^{29}\text{Si}$  respectively.  $^1\text{H}$  MAS and  $^1\text{H}$  double quantum (DQ) NMR spectra were recorded using a 5 mm MAS probe and a spinning rate of 10 kHz. A  $\pi/2$  pulse length of 3.57  $\mu\text{s}$  and a recycle delay of 5 s were used for the  $^1\text{H}$  NMR experiments. For the  $^1\text{H}$  double quantum MAS NMR experiments, DQ coherences were excited and reconverted with a POST-C7 pulse sequence<sup>32</sup> following the general scheme of two-dimensional (2D) multiple-quantum spectroscopy. The increment interval in the indirect dimension was set to 20  $\mu\text{s}$ . Typically, 128 scans were acquired for each  $t_1$  increment, and two-dimensional data sets consisted of  $128 t_1 \times$

- (14) Remy, M. J.; Stanica, D.; Poncet, G.; Feijen, E. J. P.; Grobet, P. J.; Martens, J. A.; Jacobs, P. A. *J. Phys. Chem.* **1996**, *100*, 12440–12447.
- (15) Biaglow, A. I.; Parrillo, D. J.; Kokotailo, G. T.; Gorte, R. J. *J. Catal.* **1994**, *148*, 213–223.
- (16) Pfeifer, H.; Freude, D.; Hunger, M. *Zeolites* **1985**, *5*, 274–286.
- (17) Hunger, M. *Solid State Nucl. Magn. Reson.* **1996**, *6*, 1–29.
- (18) Haw, J. F.; Nicholas, J. B.; Xu, T.; Beck, L. W.; Ferguson, D. B. *Acc. Chem. Res.* **1996**, *29*, 259–267.
- (19) Karra, M. D.; Sutovich, K. J.; Mueller, K. T. *J. Am. Chem. Soc.* **2002**, *124*, 902–903.
- (20) Kao, H. M.; Liu, H.; Jiang, J. C.; Lin, S. H.; Grey, C. P. *J. Phys. Chem. B* **2000**, *104*, 4923–4933.
- (21) Biaglow, A. I.; Gorte, R. J.; Kokotailo, G. T.; White, D. J. *J. Catal.* **1994**, *148*, 779–786.
- (22) Xu, T.; Munson, E. J.; Haw, J. F. *J. Am. Chem. Soc.* **1994**, *116*, 1962–1972.
- (23) Haw, J. F.; Xu, T.; Nicholas, J. B.; Gorguen, P. W. *Nature* **1997**, *389*, 832–835.
- (24) Xu, T.; Kob, N.; Drago, R. S.; Nicholas, J. B.; Haw, J. F. *J. Am. Chem. Soc.* **1997**, *119*, 12231–12239.
- (25) Ehresmann, J. O.; Wang, W.; Herreros, B.; Luigi, D. P.; Venkatraman, T. N.; Song, W.; Nicholas, J. B.; Haw, J. F. *J. Am. Chem. Soc.* **2002**, *124*, 10868–10874.
- (26) Yang, J.; Janik, M. J.; Ma, D.; Zheng, A.; Zhang, M.; Neurock, M.; Davis, R. J.; Ye, C.; Deng, F. *J. Am. Chem. Soc.* **2005**, *127*, 18274–18280.
- (27) Yang, J.; Zheng, A.; Zhang, M.; Luo, Q.; Yue, Y.; Ye, C.; Lu, X.; Deng, F. *J. Phys. Chem. B* **2005**, *109*, 13124–13131.
- (28) Xu, J.; Zheng, A.; Yang, J.; Su, Y.; Wang, J.; Zeng, D.; Zhang, M.; Ye, C.; Deng, F. *J. Phys. Chem. B* **2006**, *110*, 10662–10671.
- (29) Bhering, D. L.; Ramirez-Solis, A.; Mota, C. J. A. *J. Phys. Chem. B* **2003**, *107*, 4342–4347.
- (30) Mota, C. J. A.; Bhering, D. L.; Rosenbach, N., Jr. *Angew. Chem., Int. Ed.* **2004**, *43*, 3050–3053.

- (31) Freude, D.; Hunger, M.; Pfeifer, H. *J. Chem. Soc., Faraday Trans.* **1991**, *87*, 657–662.
- (32) Hohwy, M.; Jakobsen, H. J.; Eden, M.; Levitt, M. H.; Nielsen, N. C. *J. Chem. Phys.* **1998**, *108*, 2686–2694.

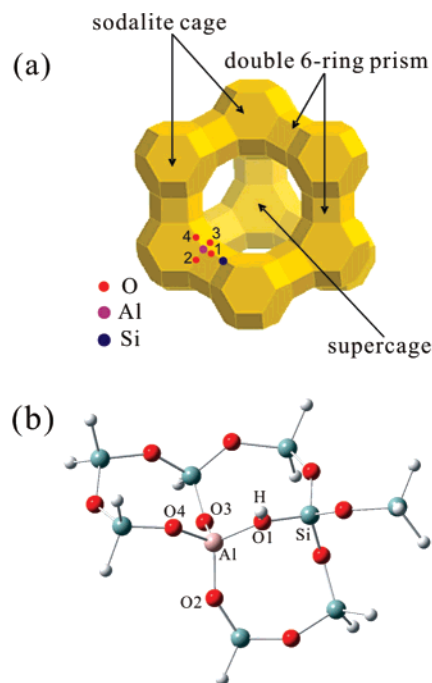


**Figure 1.** The structure of HY zeolite (a) and the selected 9T cluster model (b).

512  $t_2$ .  $^1\text{H}/^{27}\text{Al}$  TRAPDOR experiments<sup>33</sup> were carried out with a spinning speed of 10 kHz, an irradiation time of 200  $\mu\text{s}$  (two rotor periods), and a radio frequency field strength of 62.5 kHz for  $^{27}\text{Al}$ . A contact time of 2 ms, a recycle delay of 5 s, a MAS spinning speed of 6 kHz and 4000 accumulations were used for the  $^1\text{H}$ - $^{13}\text{C}$  CP/MAS measurement.  $^{29}\text{Si}$  MAS NMR spectra with high power proton decoupling were recorded using a  $\pi/4$  pulse length of 2  $\mu\text{s}$ , a recycle delay of 80 s, a spinning rate of 5 kHz, and 300 accumulations.  $^{27}\text{Al}$  MAS NMR spectra were recorded with a pulse length of 0.5  $\mu\text{s}$  ( $\leq \pi/12$ ), a recycle delay of 1 s, and a spinning rate of 6 kHz. The chemical shifts of  $^1\text{H}$ ,  $^{13}\text{C}$  and  $^{29}\text{Si}$  were externally referenced to TMS, while that of  $^{27}\text{Al}$  was referenced to 1 M aqueous  $\text{Al}(\text{NO}_3)_3$ .

**Theoretical Calculation Details.** As illustrated in Figure 1, there are two different types of cages in the faujasite-type structure: supercages and sodalite cages ( $\beta$  cages). A supercage is connected to other four supercages via a 12-ring window with a free aperture of 7.4 Å. The sodalite cages, which are connected to four adjoining supercages via a six-ring opening of 2.6 Å, are linked together by the double six-ring prisms. To theoretically investigate the Brønsted/Lewis acid synergy, a 9T cluster model consisting of three interconnected four-ring systems facing to the supercage was used to represent the framework structure of HY zeolite. The Brønsted acidic proton was located on the O1 site, and the other three nonequivalent oxygen sites such as O2, O3, and O4 were connected to the framework aluminum. Several possibly existing EFAL species such as  $\text{Al}(\text{OH})_3$ ,  $\text{AlOOH}$ ,  $\text{Al}(\text{OH})_2^+$ ,  $\text{AlO}^+$ , and  $\text{AlOH}^{2+}$  were selected to coordinate with the oxygen atom nearby the framework aluminum. To keep the cluster model neutral, as many framework aluminum atoms as necessary were used to compensate the positive charges of EFAL species. During the structure optimization, both the EFAL species and all the atoms of Brønsted acid sites in the framework were allowed to relax, while the other atoms were fixed. Each peripheral Si atom was saturated with hydrogen atoms in the calculations, and the terminal H atoms were located at a Si-H distance of 1.47 Å. No atom in the acetone molecule was constrained through all the configuration optimizations of adsorption complex models.

The geometrical parameters, single point energies for the EFAL species present in the HY zeolite were calculated at the DFT level using

(33) Grey, C. P.; Vega, A. J. *J. Am. Chem. Soc.* **1995**, *117*, 8232–8242.

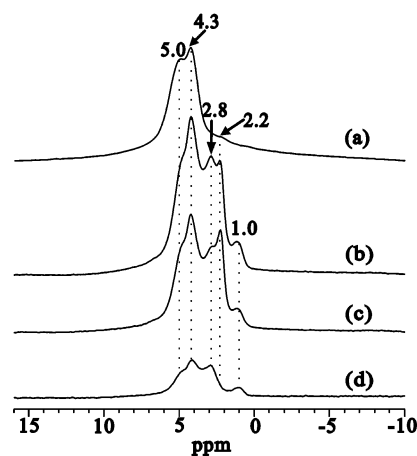


**Figure 2.**  $^1\text{H}$  single-pulse MAS spectrum of (a) HY and  $^1\text{H}$  spin-echo MAS spectra of (b) dealuminated HY (without  $^{27}\text{Al}$  irradiation), (c) dealuminated HY (with  $^{27}\text{Al}$  irradiation), and (d) difference spectra of parts b and c.

the Becke's three-parameter hybrid method with the Lee–Yang–Parr correlation functional (B3LYP) and the 6-31G\*\* basis set. While the geometrical optimization for the acetone adsorption complexes were calculated at the B3LYP/DZVP2<sup>34</sup> level, which has been demonstrated to successfully predict the structure and the NMR parameters of probe molecules adsorbed on zeolites.<sup>35</sup> The NMR parameters were calculated using the gauge independent atomic orbital (GIAO)<sup>36</sup> method at the same level of structure optimization. The calculated  $^{13}\text{C}$  NMR isotropic chemical shift of the carbonyl carbon of acetone adsorption complexes was referenced to the NMR experimental value of the gas-state acetone (208 ppm), and the calculated  $^1\text{H}$  chemical shifts were referenced to methanol whose NMR experimental value is 0.02 ppm in the gas phase.<sup>37</sup> All the calculations in this study were performed using the Gaussian03 program package.<sup>38</sup>

## Results and Discussion

**$^1\text{H}$  DQ MAS NMR.**  $^1\text{H}$  MAS NMR can provide direct information about the hydroxyl groups in zeolites. In the  $^1\text{H}$  MAS NMR spectrum of HY (Figure 2a), two major signals at 5.0 and 4.3 ppm are observable, which were unambiguously assigned by the use of deuterated pyridine as a probe molecule for bridging  $\text{SiOHAl}$  groups (Brønsted acid sites) in the sodalite and the supercage of HY zeolite, respectively.<sup>39</sup> In addition, a minor peak at 2.2 ppm due to nonacidic  $\text{SiOH}$  groups is present in the  $^1\text{H}$  MAS NMR spectrum. For the dealuminated HY (Figure 2b), two extra resonances at 2.8 and 1.0 ppm appear, which are attributable to two different types of  $\text{AlOH}$  hydroxyl groups associated with EFAL species that can act as a Lewis acid site.<sup>40</sup> Under on-resonance  $^{27}\text{Al}$  irradiation, apart from the signals at 5.0 and 4.3 ppm, the two signals at 2.8 and 1.0 ppm are largely reduced as well (see Figure 2c and 2d), indicating that the corresponding hydroxyl groups are in close proximity to aluminum.

(34) Godbout, N.; Salahub, D. R.; Andzelm, J.; Wimmer, E. *Can. J. Chem.* **1992**, *70*, 560–571.

(35) Barich, D. H.; Nicholas, J. B.; Xu, T.; Haw, J. F. *J. Am. Chem. Soc.* **1998**, *120*, 12342–12350.

(36) Wolinski, K.; Hilton, J. F.; Pulay, P. *J. Am. Chem. Soc.* **1990**, *112*, 8251–8260.

(37) Haase, F.; Sauer, J. *J. Am. Chem. Soc.* **1995**, *117*, 3780–3789.

(38) Frisch, M. J. et al. *Gaussian03*, revision B.05; Gaussian, Inc.: Pittsburgh, PA, 2003.

(39) Freude, D.; Hunger, M.; Pfeifer, H.; Schwieger, W. *Chem. Phys. Lett.* **1986**, *128*, 62–66.

(40) Jiao, J.; Altwasser, S.; Wang, W.; Weitkamp, J.; Hunger, M. *J. Phys. Chem. B* **2004**, *108*, 14305–14310.

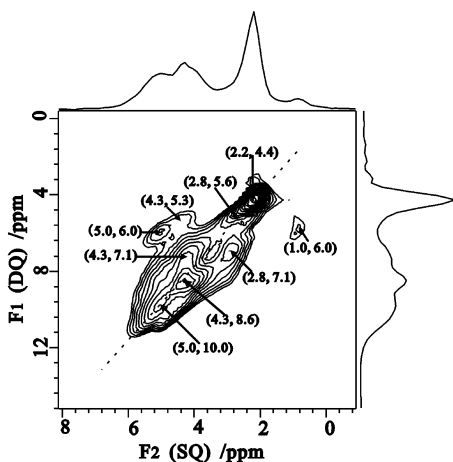


**Figure 3.**  $^1\text{H}$  DQ MAS NMR spectra of dealuminated HY.

The two-dimensional  $^1\text{H}$  DQ MAS NMR experiment is a useful method for probing proton–proton proximities in various solid materials.<sup>41</sup> Since the  $^1\text{H}$  NMR signals of dealuminated HY correspond to various hydroxyl groups that can act as different acid sites,  $^1\text{H}$  double quantum MAS NMR has been employed to investigate the spatial proximities among various acid sites in the dealuminated HY. The presence of a signal in the  $^1\text{H}$  DQ MAS spectrum indicates that two protons are in close proximity ( $<5 \text{ \AA}$ ), as the DQ coherences observed are strongly dependent on the internuclear distance. Peaks that occur along the diagonal ( $\omega, 2\omega$ ) are autocorrelation peaks resulting from the dipolar interaction of protons with the same chemical shift, while pairs of off-diagonal peaks at  $(\omega_a, \omega_a + \omega_b)$  and  $(\omega_b, \omega_a + \omega_b)$  correspond to correlations between two protons with different chemical shifts. Four autocorrelation peaks can be clearly observed in the  $^1\text{H}$  DQ MAS spectrum of dealuminated HY (Figure 3). The autocorrelation peak appearing at (4.3, 8.6) ppm suggests the spatial proximity of Brønsted acid sites in the supercage. This is consistent with the recent findings of Grey et al.<sup>42</sup> in which, by employing several probe molecules with two basic sites, they found that there were at least six pairs of Brønsted acid sites with the distance being approximately within  $6 \text{ \AA}$  in each unit cell of zeolite HY ( $n_{\text{Si}}/n_{\text{Al}} = 2.6$ ). The appearance of the autocorrelation peak at (5.0, 10.0) ppm also indicates the spatial proximity of Brønsted acid sites in the small sodalite cage. The third autocorrelation peak at (2.2, 4.4) ppm results from the dealumination process,<sup>43</sup> in which adsorbed water molecules break the Al–O bonds due to the thermal treatment for HY, releasing  $\text{Al}(\text{OH})_3$  species out of the framework and leading to the formation of a silanol nest where the silanol groups are in close proximity each other. The fourth autocorrelation peak at (2.8, 5.6) ppm is due to extra-framework  $\text{AlOOH}$  or  $\text{Al}(\text{OH})_2^{2+}$  in close proximity or EFAL species containing more than one hydroxyl group such as  $\text{Al}(\text{OH})_3$  and  $\text{Al}(\text{OH})_2^+$ . Besides the autocorrelation peaks, two intense off-diagonal peak pairs are observable as well. The off-diagonal peak pair at (1.0, 6.0) and (5.0, 6.0) ppm corresponds to the correlation between the extra-framework  $\text{AlOH}$  group (Lewis acid site) and the bridging hydroxyl group (Brønsted acid sites)

(41) Brown, S. P.; Spiess, H. W. *Chem. Rev.* **2001**, *101*, 4125–4155.

(42) Peng, L.; Chupas, P. J.; Grey, C. P. *J. Am. Chem. Soc.* **2004**, *126*, 12254–12255.

(43) Wang, Q. L.; Giannetto, G.; Torrealba, M.; Perot, G.; Kappenstein, C.; Guisnet, M. *J. Catal.* **1990**, *130*, 459–470.

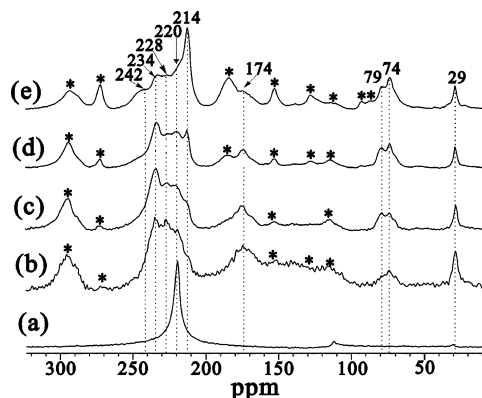


**Figure 4.**  $^{13}\text{C}$  CP/MAS NMR spectra of 2- $^{13}\text{C}$ -acetone adsorbed on HY and dealuminated HY zeolites with different loadings: (a) HY, 2.4 acetone/u.c. (unit cell); (b) dealuminated HY, 1.2 acetone/u.c.; (c) dealuminated HY, 2.4 acetone/u.c.; (d) dealuminated HY, 4.8 acetone/u.c.; (e) dealuminated HY, 7.2 acetone/u.c. Asterisks denote spinning sidebands.

in the sodalite cage, indicating the spatial proximity between the two different types of acid sites. The appearance of another off-diagonal peak pair at (2.8, 7.1) and (4.3, 7.1) ppm confirms the spatial proximity between the Lewis and the Brønsted acid sites in the supercage. On the basis of the  $^1\text{H}$  DQ MAS experiment, we can unambiguously assign the two signals at 2.8 and 1.0 ppm to the EFAL species present in the supercage and the sodalite cage, respectively. In addition, a weak off-diagonal peak at (4.3, 5.3) ppm is visible, being indicative of the spatial correlation between the Brønsted acid site in the supercage and the Lewis acid site in the sodalite cage. It is interesting that the autocorrelation peak is absent for the single-quantum signal at 1.0 ppm. This suggests that the corresponding EFAL species in the sodalite cage should exist in the form of isolated  $\text{AlOOH}$  or  $\text{Al}(\text{OH})_2^{2+}$  rather than in the form of  $\text{Al}(\text{OH})_3$  or  $\text{Al}(\text{OH})_2^+$ . Therefore, our  $^1\text{H}$  DQ MAS NMR experiments reveal the detailed spatial correlations among the various hydroxyl groups in the dealuminated HY zeolite. The spatial proximities between the Lewis and Brønsted acid sites in both the supercage and the sodalite cage are found in the dealuminated HY zeolite, implying the existence of Brønsted/Lewis acid synergy.

**$^{13}\text{C}$  NMR of Adsorbed 2- $^{13}\text{C}$ -Acetone.** 2- $^{13}\text{C}$ -Acetone is a well-established NMR probe molecule for measuring the relative Brønsted acid strengths of solid acids.<sup>20,21</sup> The formation of a hydrogen bond between the acidic proton and the carbonyl oxygen of adsorbed 2- $^{13}\text{C}$ -acetone will cause a downfield shift of the carbonyl carbon. Generally, the stronger the Brønsted acidity, the more downfield the  $^{13}\text{C}$  isotropic chemical shift. In the  $^{13}\text{C}$  NMR spectrum of 2- $^{13}\text{C}$ -acetone adsorbed on HY (Figure 4a), only one sharp resonance at ca. 220 ppm due to unreacted acetone adsorbed on the Brønsted acid site of HY is observed. Since the sodalite cage has a pore opening (the six-membered ring) of approximately  $2.6 \text{ \AA}$ , it is virtually inaccessible to the majority of adsorbed molecules including the acetone molecule with a molecular size of about  $4.5 \text{ \AA}$ .<sup>44</sup> It is expected that only the Brønsted acid site in the supercage is detectable by the 2- $^{13}\text{C}$ -acetone molecule. Figure 4b–e shows the  $^{13}\text{C}$  NMR spectra of 2- $^{13}\text{C}$ -acetone adsorbed on dealuminated HY zeolite as a function of acetone loading. Apart from the signal

(44) Kir'yakov, V. N.; Usyukin, I. P.; Shleinikov, V. M. *Chem. Technol. Fuels Oils* **1967**, *3*, 241–245.

**Table 1.** Calculated Proton Affinity (PA) and  $^1\text{H}$  Chemical Shift Data of Brønsted Acid Sites as Well as EFAL Species and  $^{13}\text{C}$  Chemical Shift Data of  $2\text{-}^{13}\text{C}$ -Acetone Adsorbed on Brønsted and Lewis Acid Sites (the Corresponding Experimental  $^1\text{H}$  and  $^{13}\text{C}$  Chemical Shifts Are Also Included)

calculated model	PA (kcal/mol)	$^1\text{H}$ chemical shift of EFAL species (ppm)		$^1\text{H}$ chemical shift of Brønsted acid site (ppm)		$^{13}\text{C}$ chemical shift of acetone adsorbed on Brønsted acid site (ppm)		$^{13}\text{C}$ chemical shift of acetone adsorbed on Lewis acid site (ppm)		existing possibility
		calcd	exptl	calcd	exptl	calcd	exptl	calcd	exptl	
HY	9T(1Al)	306.2			4.2		224.5			
	9T(2Al)	310.6			4.1	4.3	221.5	220		
	9T(3Al)	311.2			4.1		221.1			
dealuminated HY with EFAL in supercage	$\text{Al}(\text{OH})_3$	$\text{I}^a$ 319.4	2.0, 1.4, 3.8		13.9					impossible
		$\text{II}^b$ 294.8	1.4, 1.1, 1.4		4.5		232.6		241.3	possible
	$\text{AlOOH}^c$	369.8	2.7, 1.9	1.0				228		impossible
	$\text{AlO}^{+c}$	364.5	2.9						242	impossible
	$\text{Al}(\text{OH})_2^+$	301.8	3.0, 6.1		15.9					impossible
	$\text{AlOH}^{2+}$	$\text{I}^d$ 300.1	2.9		4.5	4.3	229.2		241.9	impossible
		$\text{II}^e$ 287.4	2.6		4.8		232.3		239.8	possible
dealuminated HY with EFAL in sodalite cage		$\text{III}^f$ 279.6	2.9	2.8	5.0		235.3	234	240.5	possible
	$\text{AlOH}^{2+}$	299.9	2.3		4.4		228.4			possible

<sup>a</sup>  $\text{Al}(\text{OH})_3$  coordinated to O4 site. <sup>b</sup>  $\text{Al}(\text{OH})_3$  coordinated to O2 site. <sup>c</sup> Proton transfer occurs from Brønsted acid sites to EFAL species. <sup>d</sup>  $\text{AlOH}^{2+}$  located in the 4-membered ring containing O3 and O4 sites. <sup>e</sup>  $\text{AlOH}^{2+}$  located in the 4-membered ring containing O1 and O3 sites. <sup>f</sup>  $\text{AlOH}^{2+}$  located in the 4-membered ring containing O1 and O2 sites.

at 220 ppm due to  $2\text{-}^{13}\text{C}$ -acetone adsorbed on the Brønsted acid site and signals at 214, 174, 79, 74, and 29 ppm arising from the products of bimolecular and trimolecular reactions (aldol reaction) of  $2\text{-}^{13}\text{C}$ -acetone,<sup>21</sup> three additional signals are observable at 228, 234, and 242 ppm, which can be assigned to acetone directly adsorbed on either the Al site of the EFAL species (as Lewis acid site) or the bridging OH group (as the Brønsted acid site) in spatial proximity to or having an interaction with the EFAL species. For the latter case, the larger  $^{13}\text{C}$  chemical shift of the signals indicates that the acid strength of the corresponding bridging OH groups is remarkably enhanced because of the Brønsted/Lewis acid synergy compared with that of HY zeolite (having a  $^{13}\text{C}$  chemical shift of 220 ppm). As will be seen in the following, in combination with theoretical calculation, the two  $^{13}\text{C}$  signals at 228 and 234 ppm can be attributed to acetone adsorbed on two Brønsted acid sites in close proximity to two different types of EFAL species, whereas the signal at 242 ppm to acetone directly adsorbed on the Al atom of EFAL species.

**DFT Calculations.** We use the quantum chemical calculation method to obtain detailed information about the EFAL species as well as the Brønsted/Lewis acid synergy in dealuminated HY zeolite. On the basis of the  $^1\text{H}$  DQ MAS NMR experimental result, the EFAL species are in close proximity to the Brønsted acid sites and the possible EFAL species considered in the supercage include  $\text{Al}(\text{OH})_3$ ,  $\text{AlOOH}$ ,  $\text{Al}(\text{OH})_2^+$ , and  $\text{Al}(\text{OH})^{2+}$ , whereas those in sodalite cage are  $\text{AlOOH}$  and  $\text{Al}(\text{OH})^{2+}$ . Although the EFAL species  $\text{AlO}^+$  is unable to be detected by  $^1\text{H}$  NMR, the interaction of the EFAL species with the Brønsted acid site is discussed as well. We first optimized the geometries of various acid sites and acetone adsorption complexes in both HY and dealuminated HY zeolites and then calculated the proton affinity (PA) and  $^1\text{H}$  and  $^{13}\text{C}$  chemical shifts of the corresponding system. The calculated results were listed in Table 1.

In order to investigate the acid strength of HY zeolite, a 9T(2Al) cluster having two framework aluminum was selected to represent the real structure of HY zeolite. Figure 5a shows the optimized geometry for the 9T(2Al) cluster, in which the distance between the acidic proton and the framework oxygen atom is 0.967 Å. The PA value of HY zeolite defined as the

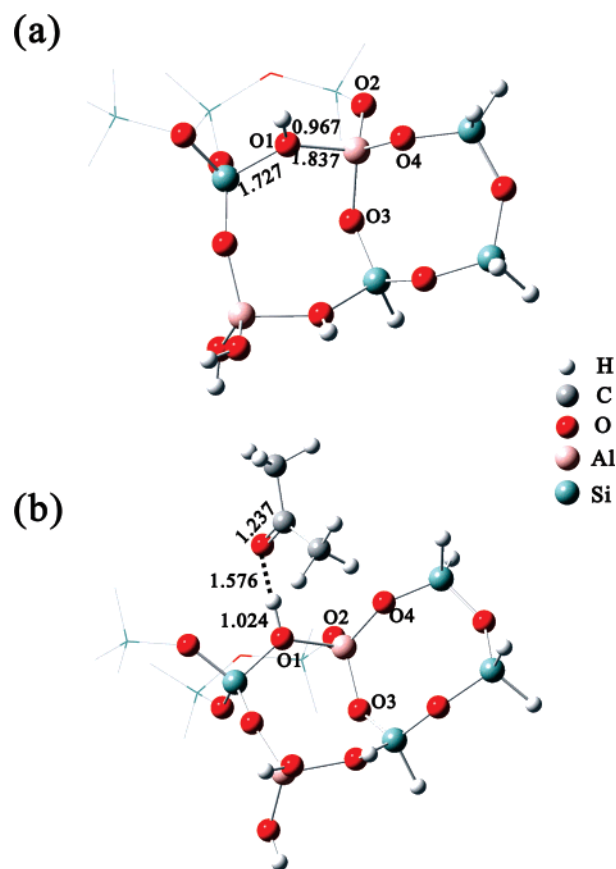


**Figure 5.** The optimized geometries of the Brønsted acid site in HY zeolite (a) and the acetone adsorption complex (b). Selected bond lengths in angstroms are indicated. For clarity, some of atoms and bonds in the 9T cluster were represented as wireframes.

energy difference between the corresponding deprotonated and protonated models was theoretically determined to be 310.6 kcal/mol after the zero point thermal energy correction. Figure 5b displays the optimized geometry of acetone adsorbed on the Brønsted acid site of HY zeolite. There is a strong hydrogen bond between the acidic proton and the carbonyl oxygen of adsorbed acetone, and the corresponding distance is 1.576 Å.

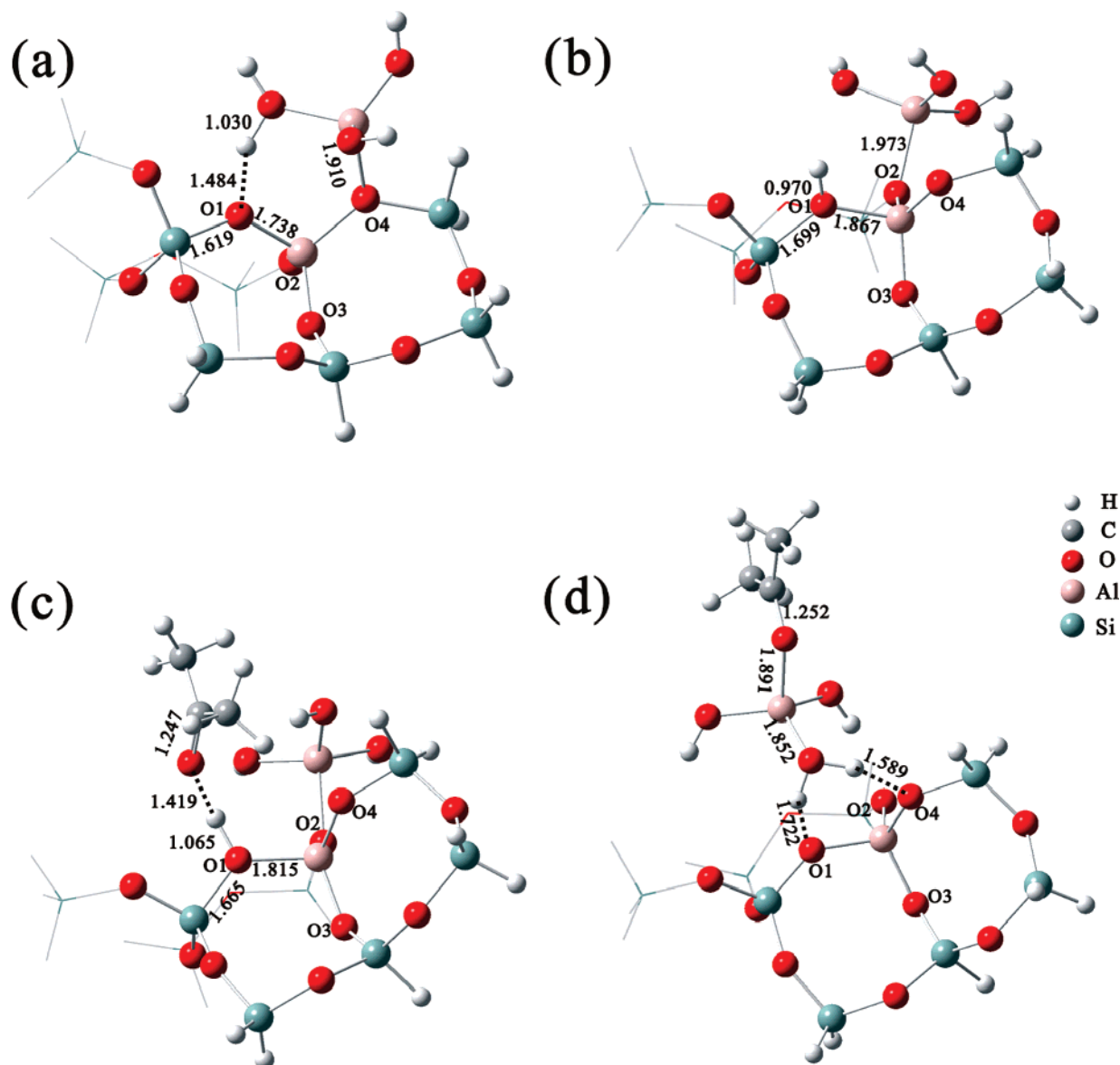


**Figure 6.** The optimized geometries of the Brønsted acid site in dealuminated HY zeolite with  $\text{Al}(\text{OH})_3$  coordinating to the framework O4 (a) and O2 (b) sites and the acetone adsorption complexes on the Brønsted (c) and Lewis (d) acid sites. Selected bond lengths in angstroms are indicated. For clarity, some of atoms and bonds in the 9T cluster were represented as wireframes.

The zeolite–OH bond length increases from 0.967 in the bare zeolite to 1.024 Å in the adsorption complex, and the C=O bond length of acetone increases from 1.224 (in free gas state) to 1.237 Å after the acetone adsorption. Using the theoretical calculation at the same computational level, we calculated the  $^1\text{H}$  chemical shift of the Brønsted acid site and the  $^{13}\text{C}$  chemical shift of acetone adsorbed on the Brønsted acid site (see Table 1). The corresponding values are 4.1 and 221.5 ppm, respectively, in good agreement with our experimental observation (4.3 and 220 ppm). The result suggests that our selected cluster model is able to represent the real structure of HY zeolite and the calculation method is reliable in predicting the  $^1\text{H}$  and  $^{13}\text{C}$  NMR chemical shifts. We also calculated the 9T cluster models having one or three framework aluminum atoms. The calculated PA values and  $^1\text{H}$  chemical shifts of the Brønsted acid site and the  $^{13}\text{C}$  chemical shifts of the acetone complexes were also list in Table 1. Obviously, the less framework aluminum in the computational model, the larger the  $^{13}\text{C}$  chemical shift of

adsorbed acetone and thus the stronger the acidity of HY zeolite. This is consistent with other calculations that show that the acid strength increases as the Brønsted acid site becomes isolated because of the dealumination process.<sup>45</sup>

One of the possible EFAL species in the supercage,  $\text{Al}(\text{OH})_3$ , was selected to coordinate to the two possible oxygen sites (O4 and O2) near the framework aluminum. The optimized structures are displayed in Figure 6a and 6b, respectively. Since the O3 site is facing the sodalite cage, the coordination between the EFAL species and the O3 site is not considered for further calculation. As shown in Figure 6a, when the  $\text{Al}(\text{OH})_3$  species coordinates to the O4 site, there is a strong hydrogen bond between the Brønsted acid site and the  $\text{Al}(\text{OH})_3$  species, and the acidic proton is nearly transferred to one of the oxygen atoms of the EFAL species. In this case, the zeolite–OH bond length has been elongated from 0.967 Å in the bare zeolite to 1.484 Å

(45) Zhidomirov, G. M.; Yakovlev, A. L.; Milov, M. A.; Kachurovskaya, N. A.; Yudanov, I. A. *Catal. Today* **1999**, *51*, 397–410.

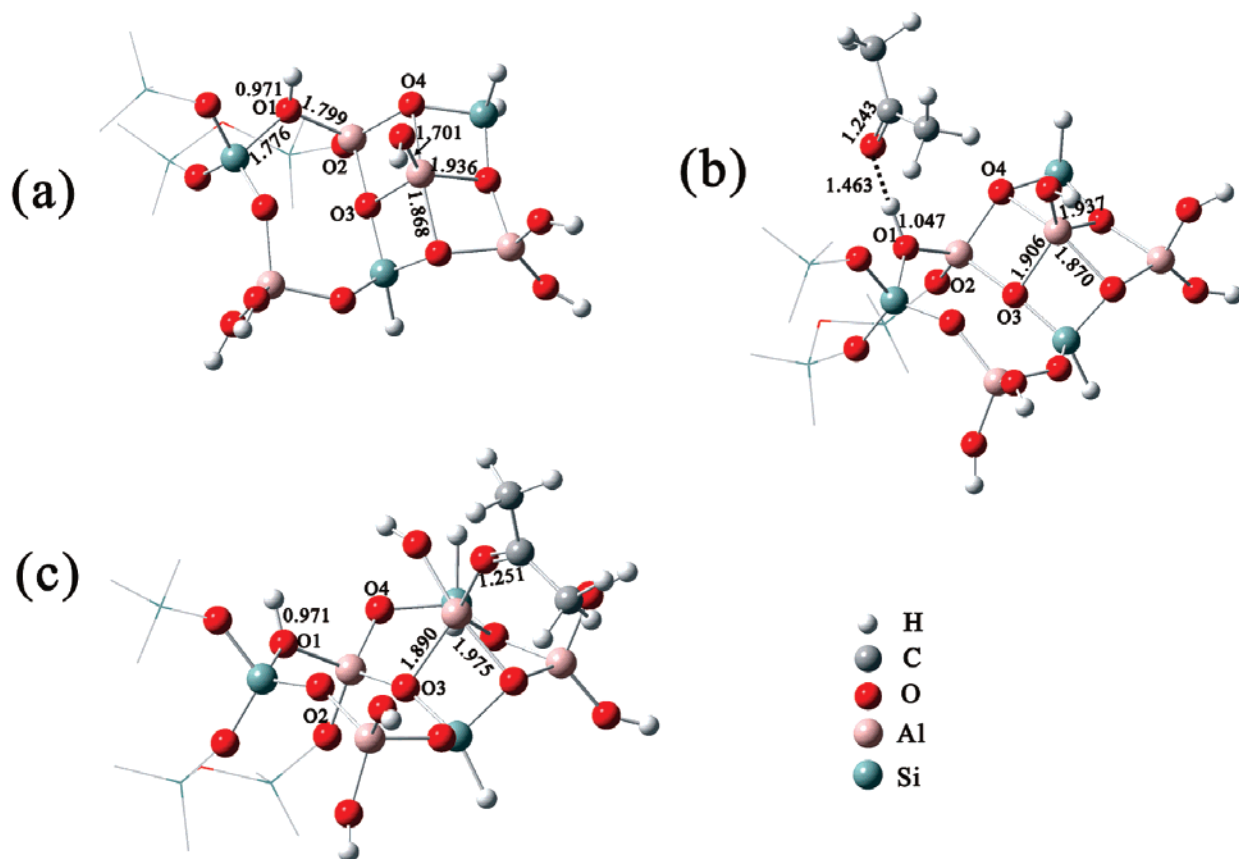


**Figure 7.** The optimized geometries of the Brønsted acid site (a) in dealuminated HY with  $\text{Al}(\text{OH})_2^+$  located in the four-membered rings containing O3 and O4 sites and the acetone adsorption complexes on the Brønsted (b) and Lewis (c) acid sites. Selected bond lengths in angstroms are indicated. For clarity, some of atoms and bonds in the 9T cluster were represented as wireframes.

in the dealuminated zeolite. The calculated PA increases to 319.4 kcal/mol compared with that (ca. 310 kcal/mol) of HY zeolite, indicating that the interaction between the  $\text{Al}(\text{OH})_3$  species and the Brønsted acid site decreases the acid strength of dealuminated HY zeolite, which is in agreement with the previous calculations in which a 6T cluster model was employed<sup>30</sup> but inconsistent with our experimental observation. In addition, it can be expected that the existence of the hydrogen bond between the Brønsted acid site and the  $\text{Al}(\text{OH})_3$  species will have a remarkable effect on the <sup>1</sup>H chemical shift of the acidic proton. We calculated the <sup>1</sup>H chemical shift and found that it was increased to 13.9 ppm because of the hydrogen-bond interaction. This result disagrees with our experimental evidence that the <sup>1</sup>H chemical shift of the acidic proton remains almost unchanged (4.3 ppm) before and after the dealumination. Therefore, it can be concluded that the coordination of the  $\text{Al}(\text{OH})_3$  species to the O4 site is unfavorable in the dealuminated HY zeolite. In a similar way, we also calculated the coordination of  $\text{Al}(\text{OH})_3$  species to the O2 site near the Brønsted acid site in the supercage, and a quite different result was obtained. As shown in Figure 6b, although there is no direct interaction (such as the hydrogen-bond interaction) between the EFAL species and the acidic proton, the zeolite–OH bond length is slightly increased from 0.967 in the HY zeolite to 0.970 Å in the dealuminated HY zeolite, and the calculated PA is reduced from 310.6 to 294.8 kcal/mol, indicating that the acid strength of dealuminated HY is increased due to the Brønsted/Lewis acid synergy. The calculated <sup>1</sup>H chemical shift of hydroxyl groups in the  $\text{Al}(\text{OH})_3$  species falls in the range of 1.1–1.4 ppm and

that of the Brønsted acid site is 4.5 ppm. The former slightly deviates from the experimental value (2.8 ppm), while the latter agrees well with our NMR experimental observation (4.3 ppm). When the acetone molecule is adsorbed on the Brønsted acid site having a synergy with the Lewis acid site (shown in Figure 6c), the zeolite–OH bond length is lengthened from 1.024 to 1.065 Å, and the C=O bond length increases from 1.237 to 1.247 Å in comparison with the acetone adsorption complex on HY zeolite. As a consequence, the calculated <sup>13</sup>C chemical shift of acetone is 232.7 ppm, much larger than that of acetone adsorbed on HY zeolite (221.5 ppm) and consistent with one of the experimental values (234 ppm). Therefore, our theoretical calculations indicate that the close proximity of  $\text{Al}(\text{OH})_3$  species to the Brønsted acid site leads to an increase in the acid strength of dealuminated HY zeolite. As shown in Figure 6d, when the acetone molecule is directly complexed with the Al atom of  $\text{Al}(\text{OH})_3$  species (the Lewis acid site), the acidic proton is transferred to the EFAL species, and the C=O bond length is further elongated to 1.252 Å. In this case, the <sup>13</sup>C chemical shift of adsorbed acetone is calculated to be 241.9 ppm, similar to our experimental result (242 ppm). The good agreement between the experimental observations and the theoretical calculations indicates that the  $\text{Al}(\text{OH})_3$  species is one of the most preferred EFAL species (Lewis acid site) present in dealuminated HY zeolite, and the coordination of the EFAL species to the O2 site near the Brønsted acid site in the supercage results in the enhanced acidity.



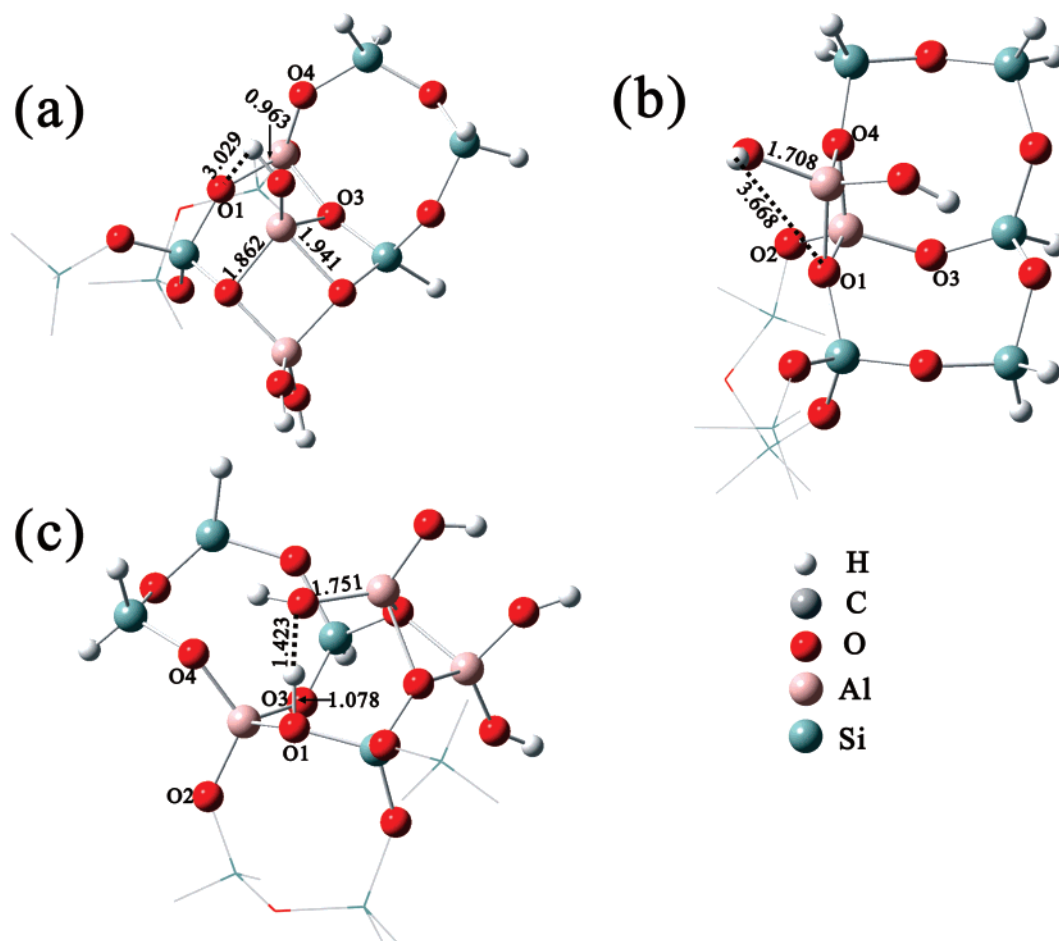


**Figure 8.** The optimized geometries of the Brønsted acid site in dealuminated HY zeolite having an interaction with (a)  $\text{AlO}^+$ , (b)  $\text{AlOOH}$ , and (c)  $\text{Al}(\text{OH})_2^+$ . Selected bond lengths in angstroms are indicated. For clarity, some of atoms and bonds in the 9T cluster were represented as wireframes.

Figure 7a shows the optimized geometries of the Brønsted acid site in close proximity to the  $\text{AlOH}^{2+}$  species in the supercage. In this case, the EFAL species is located in the four-membered ring containing the O3 and O4 sites. There is no direct interaction (such as the hydrogen-bond interaction) between the acidic proton and the EFAL species. In comparison with the HY zeolite, the O–H bond length increases to 0.971 Å, and the corresponding calculated PA is reduced to 300.1 kcal/mol. The calculated  $^1\text{H}$  chemical shifts (2.9 and 4.5 ppm) of both the  $\text{AlOH}^{2+}$  species and the Brønsted acid site are in good agreement with our NMR experimental observation (2.8 and 4.3 ppm). As shown in Figure 7a, the  $\text{AlOH}^{2+}$  species coordinating to O3 and O4 sites are in 5-fold oxygen coordination. In a recent study of the dealuminated zeolite HY, Jiao et al. found that the appearance of  $^{27}\text{Al}$  NMR signal at about 35 ppm could be an indication of a 5-fold oxygen coordination of extra-framework species.<sup>46</sup> When the acetone molecule is adsorbed on the Brønsted acid site (shown in Figure 7b), the zeolite–OH and the C=O bond lengths are elongated to 1.047 and 1.243 Å, respectively, and the calculated  $^{13}\text{C}$  chemical shift of adsorbed acetone increases to 229.2 ppm, similar to one of the NMR experimental values (228 ppm). Such a large value for the  $^{13}\text{C}$  NMR chemical shift also indicates that the acid strength of the Brønsted acid site in close proximity to  $\text{AlOH}^{2+}$  species is apparently enhanced because of the Brønsted/Lewis

acid synergy. When the acetone molecule is directly coordinated to the Al atom of  $\text{AlOH}^{2+}$  species (Figure 7c), the zeolite–OH bond length remains almost unchanged, while the C=O bond length of adsorbed acetone is elongated to 1.251 Å. The calculated  $^{13}\text{C}$  chemical shift of the carbonyl carbon of acetone molecule is 242.1 ppm, being in good agreement with our NMR observation (242 ppm). We also considered the cases where the  $\text{AlOH}^{2+}$  species is located in the other two four-membered rings (containing either the O1 and O3 sites or the O1 and O2 sites). The calculated results are listed in Table 1 (also see Supporting Information). In the two cases, the acid strength of the Brønsted acid site in close proximity to  $\text{AlOH}^{2+}$  species is further enhanced, which is demonstrated by the fact that the calculated PA values are further reduced to 287.4 and 279.6 kcal/mol, and the calculated  $^{13}\text{C}$  chemical shifts are increased to 232.3 and 235.3 ppm, respectively. In addition, it is noteworthy that no hydrogen-bond interaction is present between the acidic proton and the EFAL species. When the acetone molecule is directly coordinated to the Lewis acid sites, the calculated  $^{13}\text{C}$  chemical shifts of the carbonyl carbon are 239.8 and 240.5 ppm, respectively. All the calculated chemical shift data agree well with our NMR experimental observations as well. Therefore, it is reasonable to conclude that the  $\text{AlOH}^{2+}$  species is another one of the most preferred EFAL species (Lewis acid site) present in dealuminated HY zeolite.

Figure 8 shows the optimized structures of Brønsted acid sites having an interaction with the  $\text{AlO}^+$ ,  $\text{AlOOH}$ , and  $\text{Al}(\text{OH})_2^+$

(46) Jiao, J.; Kanellopoulos, J.; Wang, W.; Ray, S. S.; Foerster, H.; Freude, D.; Hunger, M. *Phys. Chem. Chem. Phys.* **2005**, *7*, 3221–3226.

species in the supercage. In the cases of  $\text{AlO}^+$  and  $\text{AlOOH}$  coordinating to the oxygen atom near the framework aluminum (Figure 8a and 8b), the acidic proton is transferred from the Brønsted acid site to the oxygen atom of EFAL species, resulting in the formation of  $\text{AlOH}^{2+}$  and  $\text{Al}(\text{OH})_2^+$  species, respectively. Obviously, these two EFAL species are more stable than  $\text{AlO}^+$  and  $\text{AlOOH}$ . The calculated PA values of the two systems are remarkably increased, being indicative of a decrease in the Brønsted acidity and thus no Brønsted/Lewis acid synergy. The result is consistent with the previous theoretical work<sup>30</sup> but disagrees with our NMR experiments. In the case of  $\text{Al}(\text{OH})_2^+$  coordinating to the oxygen atom near the framework aluminum (Figure 8c), a hydrogen bond is formed between the acidic proton and the oxygen atom of  $\text{Al}(\text{OH})_2^+$ . The existence of the hydrogen bond results in the calculated  $^1\text{H}$  chemical shift of acidic proton moving to 15.9 ppm, which also disagrees with our NMR observation. Therefore, it is conceivable that the presence of the three EFAL species ( $\text{AlO}^+$ ,  $\text{AlOOH}$ , and  $\text{Al}(\text{OH})_2^+$ ) is not likely in the dealuminated HY zeolite based on our theoretical calculations and NMR experiments.

Since our  $^1\text{H}$  DQ MAS NMR experiment also provides evidence that the Brønsted acid site in the supercage is in close proximity to the EFAL species (in the form of either  $\text{AlOH}^{2+}$  or  $\text{AlOOH}$ ) in the sodalite cage, we also calculated the corresponding Brønsted/Lewis acid synergy. As shown in the calculations, the EFAL species with an  $\text{Al}=\text{O}$  bond such as in  $\text{AlOOH}$  is unstable in dealuminated HY zeolite. Thus, only the  $\text{AlOH}^{2+}$  species present in the sodalite cage is taken into account for further calculation. The optimized geometries (Figure 9) show that the O–H bond length is increased to 0.971 Å and the corresponding PA value is 299.9 kcal/mol, which is smaller than that of HY zeolite. As displayed in Table 1, both the calculated  $^1\text{H}$  NMR chemical shift (4.4 ppm) of the Brønsted acid site and the calculated  $^{13}\text{C}$  NMR chemical shift (228.4 ppm) of adsorbed acetone agree well with our NMR observations (4.5 and 228 ppm). Compared with the HY zeolite, the larger  $^{13}\text{C}$  chemical shift of adsorbed acetone suggests that the presence of  $\text{AlOH}^{2+}$  in the sodalite cage can also enhance the acidity of the neighboring Brønsted acid site in the supercage even though there is no direct interaction between them.

**Lewis Acid and Its Synergy with the Brønsted Acid.** It is generally accepted that the Lewis acid sites in zeolites are associated with EFAL species and play an important role in the zeolite-mediated hydrocarbon reactions. Although  $^{27}\text{Al}$  MAS NMR spectroscopy has been extensively used to characterize the nature of EFAL species,<sup>47–50</sup> its detailed structure remains to be fully understood. The EFAL species is hypothesized to be oxoaluminum ions and some neutral species. Our experimental and theoretical calculation results can allow us to determine the detailed structure of EFAL species in dealuminated HY zeolite. The most preferred EFAL species in the supercage is either  $\text{Al}(\text{OH})_3$  or  $\text{Al}(\text{OH})_2^+$ , while  $\text{Al}(\text{OH})_2^+$  is the only candidate in the sodalite cage. As long as the structure of the EFAL species is known, more research work may be

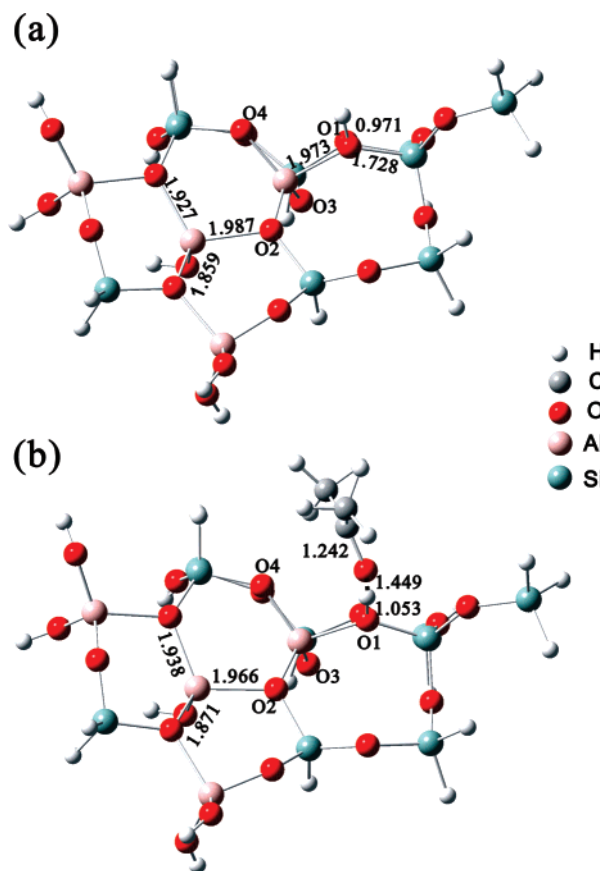
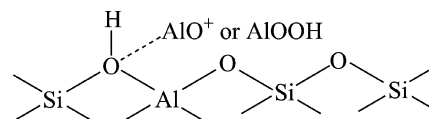


**Figure 9.** The optimized geometries of the Brønsted acid site (a) in the supercage of dealuminated HY zeolite with  $\text{AlOH}^{2+}$  coordinating to the oxygen atom nearest the framework aluminum in the sodalite cage, and the acetone adsorption complex (b) on the Brønsted acid site. Selected bond lengths in angstroms are indicated.

expected to explore the interaction of EFAL species with reactant molecules, which would lead to a good understanding of the role of EFAL species in the zeolite-related catalytic reactions.

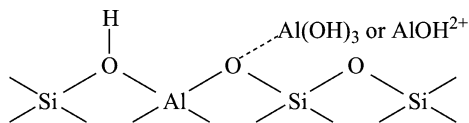
The acidity enhancement from the interactions between a framework Brønsted site and an extra-framework Lewis site in zeolites has been suggested since the 1980s,<sup>7</sup> and such a view is now generally recognized. A simplified representation of the interaction is as follows:



As pointed out by Mirodatos et al.,<sup>7</sup> the interaction will involve a partial electron transfer from the OH bond to the oxoaluminum species (such as  $\text{AlO}^+$  and  $\text{AlOOH}$ ), which would increase the acid strength of the site by decreasing the OH bond strength, similar to that occurring in the superacid systems such as  $\text{AlCl}_3\text{--HCl}$  and  $\text{SbF}_5\text{--HF}$ . If such a proposal was correct, the  $^1\text{H}$  chemical shift of the Brønsted acid site would be expected to move downfield. Indeed, the  $^1\text{H}$  chemical shift almost remains constant in either the presence or the absence of EFAL species. Our NMR experiments in combination with DFT calculations indicate a different mechanism of Brønsted/Lewis acid synergy. The coordination of the Lewis acid site ( $\text{Al}(\text{OH})_3$  or  $\text{Al}(\text{OH})_2^+$ ) to the oxygen atom nearest to the Brønsted acid site is capable

- (47) Deng, F.; Yue, Y.; Ye, C. *J. Phys. Chem. B* **1998**, *102*, 5252–5256.  
 (48) van Bokhoven, J. A.; Koningsberger, D. C.; Kunkeler, P.; van Bekkum, H.; Kentgens, A. P. M. *J. Am. Chem. Soc.* **2000**, *122*, 12842–12847.  
 (49) Fyfe, C. A.; Bretherton, J. L.; Lam, L. Y. *J. Am. Chem. Soc.* **2001**, *123*, 5285–5291.  
 (50) van Bokhoven, J. A.; Roest, A. L.; Koningsberger, D. C.; Miller, J. T.; Nachtgaal, G. H.; Kentgens, A. P. M. *J. Phys. Chem. B* **2000**, *104*, 6743–6754.

of causing an enhanced acidity though there is no direct interaction between them (see the following).



It can be found from the optimized structures that neither the Si–OH–Al bond angle nor the Si–O and Al–O bond length of the Brønsted acid site exhibits a regular trend of variation, but the zeolite–OH bond length is found to be increased by 0.003–0.004 Å after the coordination of EFAL species. Our theoretical calculation results (see Table 1) suggest that the PA value of dealuminated HY is decreased by ca. 10–30 kcal/mol due to the Brønsted/Lewis acid synergy. The variation of both the OH bond length and the PA value indicates an enhancement of Brønsted acidity of dealuminated HY zeolite. Both our experimental and predicted  $^{13}\text{C}$  chemical shifts of acetone adsorption complexes can resolve two kinds of Brønsted acid sites in close proximity to two different types of Lewis acid sites ( $\text{Al}(\text{OH})_3$  and  $\text{Al}(\text{OH})^{2+}$ ). The increased  $^{13}\text{C}$  chemical shifts (228 and 234 ppm) indicate that their Brønsted acidity is much stronger than the non-dealuminated HY (having a  $^{13}\text{C}$  chemical shift of 220 ppm), similar to  $\text{SO}_4^{2-}/\text{ZrO}_2$  and  $\text{MoO}_x/\text{ZrO}_2$  catalysts, where adsorbed 2- $^{13}\text{C}$ -acetone gives rise to a  $^{13}\text{C}$  chemical shift in the range of 228–230 ppm,<sup>28,51</sup> but still weaker than 100%  $\text{H}_2\text{SO}_4$ , in which the isotropic chemical shift of 2- $^{13}\text{C}$ -acetone is 245 ppm.<sup>35</sup> For acetone directly adsorbed on the Lewis acid site, the experimentally observed  $^{13}\text{C}$  chemical shift (242 ppm) is close to that (245 ppm) of acetone adsorbed on a true solid superacid  $\text{AlCl}_3$ ,<sup>35</sup> being indicative of a very strong Lewis acidity of the  $\text{Al}(\text{OH})_3$  and  $\text{Al}(\text{OH})^{2+}$  species.

Carbocations were usually considered as reaction intermediates in numerous zeolite-catalyzed hydrocarbon reactions. Until the early 1990s, zeolites were believed to possess superacidity that is able to fully protonate reactants, forming carbocations persistent inside the zeolite cages. However, the early attempts of Haw and co-workers to verify the formation of simple alkyl carbocations in zeolites by solid-state NMR failed.<sup>52–55</sup> As a result of their following systematic study of carbenium ion formation, zeolites were reclassified as strong acids with acidity much lower than 100% sulfuric acid.<sup>56,57</sup> By 1998 only three types of carbenium ions as persistent species in acidic zeolites were identified by Haw et al., which include alkyl-substituted cyclopentenyl cations,<sup>52</sup> methylindanyl carbenium ions,<sup>58</sup> and *gem*-dimethylbenzenium cations.<sup>59</sup> A PA value of 209 kcal/mol was predicted with the help of DFT calculations as the lower limit for formation of a persistent carbenium ion in an

unmodified zeolite.<sup>60</sup> Since the works were almost carried out on non-dealuminated acidic zeolites, neither the role of Lewis site nor its synergy with neighboring Brønsted site was taken into account. Recently, Bjørgen et al.<sup>61,62</sup> provided clear evidence from FTIR and UV–vis spectroscopy that hexamethylbenzenium and 1,2,4,5-tetramethylbenzenium ions were formed inside the micropores of dealuminated H-beta zeolite. Hunger et al.<sup>63</sup> also observed the formation of hexamethylbenzenium ions in dealuminated H-ZSM-5 zeolite and found that almost no carbenium ion was detectable under the same reaction condition in non-dealuminated zeolite H-ZSM-5. On the basis of the lower PA limit, hexamethylbenzene (PA = 206 kcal/mol) and 1,2,4,5-tetramethylbenzene (PA = 194 kcal/mol) are too weak to be fully protonated by acidic zeolites. Apart from the steric constraints imposed by the zeolite framework which can stabilize a confined cation, we believe that Lewis acid and its synergy with the Brønsted acid may play a crucial role in the formation of the methylbenzenium ions. The present Brønsted/Lewis acid synergy model is useful for studying the guest–host interaction as well as the formation of carbenium ions in dealuminated zeolites. Our experimental and theoretical calculation results also demonstrate that the acidity of dealuminated HY zeolite is remarkably enhanced due to the Brønsted/Lewis acid synergy. Therefore, more long-lived carbenium cations with their conjugate compounds being less basic (PA < 209 kcal/mol) may be expected to form inside the micropores of dealuminated zeolites.

This work opens up a new window for investigating the role of Lewis acid and the Brønsted/Lewis acid synergy in numerous hydrocarbon reactions occurring in dealuminated zeolites. Further work on a wider range of zeolite topologies and with varying Si/Al ratios is currently under way.

## Conclusions

In summary, the Brønsted/Lewis acid synergy in dealuminated HY zeolite was studied using solid-state NMR techniques in combination with DFT quantum chemical calculations.  $^1\text{H}$  DQ MAS NMR results revealed the detailed spatial proximities between the Lewis and Brønsted acid sites in dealuminated HY zeolite.  $^{13}\text{C}$  NMR of adsorbed 2- $^{13}\text{C}$ -acetone demonstrated a remarkable increase in the acid strength of dealuminated HY zeolite due to the Brønsted/Lewis acid synergy, which was further confirmed by our theoretical calculations. With both NMR experiments and DFT calculations, the detailed structure of EFAL species and the mechanism of Brønsted/Lewis acid synergy were identified. Extra-framework  $\text{Al}(\text{OH})_3$  and  $\text{AlOH}^{2+}$  species in the supercage as well as  $\text{AlOH}^{2+}$  species in the sodalite cage are the preferred Lewis acid sites in the dealuminated HY zeolite. The coordination of the EFAL species to the oxygen atom nearest to the framework aluminum results in the enhanced acidity of the Brønsted acid site. It is noteworthy that no direct interaction (such as the hydrogen-bond interaction) exists between the EFAL species and the Brønsted acid site and they are only in close proximity. We believe that the Brønsted/Lewis acid synergy model presented here is useful for

(51) Haw, J. F.; Zhang, J.; Shimizu, K.; Venkatraman, T. N.; Luigi, D. P.; Song, W.; Barich, D. H.; Nicholas, J. B. *J. Am. Chem. Soc.* **2000**, *122*, 12561–12570.

(52) Haw, J. F.; Richardson, B. R.; Oshiro, I. S.; Lazo, N. L.; Speed, J. A. *J. Am. Chem. Soc.* **1989**, *111*, 2052–2058.

(53) Richardson, B. R.; Lazo, N. D.; Schettler, P. D.; White, J. L.; Haw, J. F. *J. Am. Chem. Soc.* **1990**, *112*, 2886–2891.

(54) Munson, E. J.; Xu, T.; Haw, J. F. *J. Chem. Soc., Chem. Commun.* **1993**, 75–76.

(55) Xu, T.; Zhang, J.; Munson, E. J.; Haw, J. F. *J. Chem. Soc., Chem. Commun.* **1994**, 2733–2735.

(56) Haw, J. F.; Nicholas, J. B.; Xu, T.; Beck, L. W.; Ferguson, D. B. *Acc. Chem. Res.* **1996**, *29*, 259–267.

(57) Haw, J. F. *Phys. Chem. Chem. Phys.* **2002**, *4*, 5431–5441.

(58) Xu, T.; Haw, J. F. *J. Am. Chem. Soc.* **1994**, *116*, 10188–10195.

(59) Xu, T.; Barich, D. H.; Goguen, P. W.; Song, W.; Wang, Z.; Nicholas, J. B.; Haw, J. F. *J. Am. Chem. Soc.* **1998**, *120*, 4025–4026.

(60) Nicholas, J. B.; Haw, J. F. *J. Am. Chem. Soc.* **1998**, *120*, 11804–11805.

(61) Bjørgen, M.; Bonino, F.; Kolboe, S.; Lillerud, K.-P.; Zecchina, A.; Bordiga, S. *J. Am. Chem. Soc.* **2003**, *125*, 15863–15868.

(62) Bjørgen, M.; Bonino, F.; Arstad, B.; Kolboe, S.; Lillerud, K.-P.; Zecchina, A.; Bordiga, S. *ChemPhysChem.* **2005**, *6*, 232–235.

(63) Hunger, M.; Wang, W. *Chem. Commun.* **2004**, 584–585.

studying the mechanism of numerous hydrocarbon reactions occurring in dealuminated zeolites.

**Acknowledgment.** We are grateful for the support of the National Natural Science Foundation of China (20425311 and 20673139). We also thank Prof. Huiru Tang of Wuhan Institute of Physics and Mathematics for critical reading of the manuscript. Parts of the calculations were performed in the Shanghai Supercomputer Center (SSC) of China.

**Supporting Information Available:**  $^{27}\text{Al}$  MAS NMR spectra of HY and dealuminated HY zeolites, optimized geometries of Brønsted acid sites and adsorption complexes with  $\text{Al}(\text{OH})^{2+}$  located in the other two four-membered rings, and complete ref 38. This material is available free of charge via the Internet at <http://pubs.acs.org>.

JA072767Y